JOURNAL OF CATALYSIS 145, 141–150 (1994)

Chromia Supported on Titania

II. Morphological Properties and Catalytic Behavior in the Selective Reduction of Nitric Oxide by Ammonia

J. Engweiler,* J. Nickl,* A. Baiker,*[1] K. Köhler,† C. W. Schläpfer,† and A. von Zelewsky†

*Department of Chemical Engineering and Industrial Chemistry, Swiss Federal Institute of Technology, ETH-Zentrum, CH-8092 Zürich, Switzerland; and †Institute of Inorganic and Analytical Chemistry, University of Fribourg, Pérolles, CH-1700 Fribourg, Switzerland

Received March 8, 1993; revised June 4, 1993

The chemical and structural properties of chromia on titania have been investigated after different pretreatments and after use for the low temperature selective catalytic reduction (SCR) of NO by NH_3. A series of catalysts containing 0.5 to 30 wt% chromia was prepared by impregnation with aqueous chromium nitrate solution. The catalysts exhibited high activity for SCR in the low temperature range (T < 470 K). The NO conversion rate was proportional to the chromia loading up to 5 wt%. Higher loadings resulted in a less efficient use of the chromia species. Selectivities to N_2 and N_2O were not influenced by the amount of deposited chromia at higher loadings (≥5 wt%), but depended markedly on the pretreatment of the catalysts. Oxidative pretreatment at 573 K for 3 h led to enhanced formation of undesired N_2O, whereas previous exposure to a H_2-containing atmosphere at T < 720 K yielded selectivities ot N_2 exceeding 90%. The overall conversion of NO was comparatively little influenced by these pretreatments. Thermal analysis (TG, DTA) and temperature-programmed reduction indicated the formation of Cr(III) species upon reduction in the H_2-containing atmosphere at 720 K. These species were reoxidizable in air at 670 K and probably highly hydroxylated, as indicated by the substantial formation of water during the thermoanalytical run. Exposure to higher temperatures (>720 K) in an inert or a hydrogen-containing atmosphere led to the formation of less active α-Cr_2O_3 which was not reoxidizable under similar conditions. Electron paramagnetic resonance (EPR) measurements of catalysts exposed to SCR conditions indicated uniformly sized clusters of Cr(III) together with Cr(V) surface species. After oxidative pretreatment and SCR use, EPR revealed the existence of Cr(I) species, probably present as $\{CrNO\}^{2+}$ surface complexes. Such species were not observed after reductive pretreatment of the catalysts.

INTRODUCTION

The selective catalytic reduction (SCR) of nitric oxide with ammonia in excess oxygen has gained considerable importance due to its efficiency. In the search for highly efficient catalysts various materials have been examined (1). The most intensively studied catalysts are based on vanadia/titania, while other oxides have received considerably less attention. Chromia-containing catalysts have been investigated for SCR by several authors (2–4). The significant N_2O production above 470 K made the chromia-based catalysts unsuitable for technical applications. However, recently we have shown that amorphous chromia exhibits interesting properties for low temperature SCR of NO (5). The amorphous chromia was found to reduce NO selectively to N_2, whereas with crystalline chromia formation of N_2 and N_2O occurred together with significant NH_3 oxidation (6). This difference in catalytic behavior has been attributed to the fact that the labile oxygen or crystalline chromia is more weakly bound than that on amorphous chromia, and therefore desorbs from the surface at lower temperature. The higher activity of amorphous chromia in SCR has been attributed to the higher density of labile oxygen available on the surface under reaction conditions (7–10).

Upon deposition of chromia on a support, its surface structure and reduction behavior may change significantly. It has been demonstrated that Cr(VI) can be stabilized on SiO_2 (11), Al_2O_3 (12), and TiO_2. For CrO_x/Al_2O_3 a stronger interaction of the Cr(VI) oxide species with the support was found than for CrO_x/TiO_2 (13). With this in mind we have extended our previous studies to titania-supported systems.

Structural and chemical changes induced by the different preparation steps studied by EPR have been reported in Part I of this series (14). After calcination at 573 K, using pure oxygen, Cr_2O_3 clusters of different sizes were found to coexist with Cr(V) and Cr(VI) surface species. For low Cr contents Cr(V) and Cr(VI) were found to be predominant, whereas for higher Cr contents (>5 wt%), the existence of antiferromagnetic α-Cr_2O_3

---

[1] To whom correspondence should be addressed.

0021-9517/94 $5.00

(and ferromagnetic CrO_2) crystallites on the surface was proposed.

Here we focus on the catalytic behavior of these catalysts and the structural changes resulting from different pretreatments and exposure to SCR conditions.

EXPERIMENTAL

Catalyst Preparation

The preparation of titania-supported chromia catalysts has been described in detail in Part I (14). Titania P25 (Degussa) was impregnated in an aqueous solution of $Cr(NO_3)_3 \cdot 9H_2O$ (Fluka) and subsequently dried. To avoid undesired crystallization of α-Cr_2O_3 during preparation, calcination was carried out under an oxygen atmosphere at 573 K. Samples with chromia contents of 0.5, 1, 2, 3, 5, 10, and 30 wt%, referred to wt% Cr_2O_3 per total catalyst mass (TiO_2 and Cr_2O_3), were prepared.

Two reference catalysts were used in the catalytic tests: these were a vanadia/titania catalyst prepared by grafting of vanadyl alkoxide according to the procedure reported in Ref. (15), referred to as V_2O_5/TiO_2, and an amorphous chromia sample described in Ref. (6).

Catalyst Characterization

Temperature-programmed reduction (TPR). The apparatus used for TPR measurements has been described in detail elsewhere (16). The measurements were carried out using 6% hydrogen in argon as reductant gas and a flow rate of 75 ml (STP) min^{-1}. Sample weights were between 0.2 and 0.5 g, depending on the chromia content. Granules of 300–500 μm were used. The temperature was ramped from 298 to 973 K at 10 K min^{-1}.

Thermoanalytical studies. Differential thermal analysis (DTA) and thermogravimetry (TG) measurements were performed on a Netzsch STA 409 instrument, using 20–50 mg of sample and a heating rate of 10 K min^{-1}. Samples of 10 wt% chromia/titania were used for the measurements. Runs were performed under a pure Ar atmosphere (30 cm^3 min^{-1}) and under Ar that contained 6% H_2 (60 cm^3 min^{-1}). α-Al_2O_3 was used as a reference material. Gases evolving during thermal analysis were monitored with a Balzers QMG 424 mass spectrometer.

EPR measurements. EPR spectra were recorded on a Bruker ESP300 system at X-band frequency (or a Varian E-9 spectrometer at Q-band frequency) at temperatures between 77 and 293 K. The spectra were measured at a microwave frequency of about 9.4 GHz for X-band (or 35.0 GHz for Q-band), with microwave powers of 1–5 mW, a modulation amplitude of 0.2 mT, and a modulation frequency of 100 kHz. For more details, see Part I (14). Measurements after exposure to SCR reaction conditions are included in this study.

Catalytic Tests

Catalytic tests were carried out in a continuous flow tubular fixed-bed microreactor. The reaction gas mixture consisted of 900 ppm NO, 900 ppm NH_3, and 1.8% O_2 with a balance of argon. This gas mixture, which is referred to as the SCR feed, was mixed from argon (99.999%) and single component gases in a balance of argon (3600 ppm NO/Ar, NH_3/Ar certified by ±2%, Union Carbide). Feed and product concentrations of NO, NO_2, NH_3, H_2O, N_2O, O_2, and N_2 were quantitatively analyzed using a computer-controlled Balzers quadrupole mass spectrometer QMA 112A. Details of the apparatus have been described elsewhere (6).

Volumes of 0.09–0.11 cm^3 corresponding to 80–140 mg of catalyst sieved to 300–500 μm particle size were used for the measurements. If not specially mentioned, the calcined catalysts (O_2, 3 h, 573 K) were used for the catalytic tests without further pretreatment. Additionally, samples containing 5 wt% Cr_2O_3 were pretreated in 6% H_2/Ar at 653 or 723 K, or subsequently heated to 873 K in Ar before activity measurements.

Conversion measurements as a function of temperature were carried out at a gas hourly space velocity (GHSV) of 24,000 (N m^3 h^{-1}) m_{cat}^{-3} after steady-state SCR activity had been established at 423 K (typically after 2 h). For activity measurements the space velocity was gradually raised to 100,000 h^{-1} and the temperature was adjusted to keep the NO conversion below 20%, which was found to be suitable for maintaining differential reactor conditions. Selectivities to N_2 and N_2O are defined as $S_i = 2 \cdot F_i/(F_{NO,in} + F_{NH3,in} - F_{NO,out} - F_{NH3,out})$, where F_i is the molar flow-rate (mol/s) of species i (N_2 or N_2O) at the reactor outlet and the subscripts "in" and "out" indicate the flow rates of NO and NH_3 at the reactor inlet and outlet, respectively. Both reactants, which were equimolarly mixed in the SCR feed, were taken into account because of the uncertain stoichiometry of the reactions leading to N_2 and N_2O formation, respectively (17).

For all measurements a nitrogen balance including feed and product stream concentrations of all N-containing compounds was calculated. Even for high conversions of NO and NH_3, the error in the N-balance did not exceed ±5%.

RESULTS

Properties of Calcined Catalysts

Properties of the calcined catalysts are listed in Table 1. The BET surface areas of all titania-supported samples were within 47 ± 2 m^2 g^{-1}, indicating that the textural properties of the titania support did not markedly change by the impregnation. This was further confirmed by pore size distribution measurements using the BJH method

TABLE 1

Catalyst Properties

Sample	S_{BET} ($m^2 g^{-1}$)	$CrO_{1.5}$ loading (μmol g^{-1})	$CrO_{1.5}$ loading (μmol m_{BET}^{-2})	H_2-TPR (μmol g^{-1})	TPR (ΔOS CrO_x)
0.5 wt% Cr_2O_3/TiO_2	47	66	1.4	75	2.3
1 wt%	48	131	2.7	178	2.7
2 wt%	46	260	5.7	295	2.2
3 wt%	45	390	8.9	452	2.4
5 wt%	49	650	13	799	2.6
10 wt%	48	1300	27	785	1.2
30 wt%	49	3950	80	1271	0.64
Amorphous Cr_2O_3	248	13,160	—	3448[a]	0.52[a]
Crystalline Cr_2O_3	86	13,160	—	184[a]	0.03[a]
V_2O_5/TiO_2	45		5.3[b]		

Note. H_2-TRP (μmol g^{-1}) represents total hydrogen consumption during TPR; TPR (ΔOS CrO_x) represents hydrogen consumption expressed as average decrease of oxidation state.

[a] Taken from Ref. (6).

[b] $VO_{2.5}$ respectively, determined by consumption of hydrogen during TPR.

(18). The chromia loadings are given in wt% chromia out of total catalyst weight assuming that all chromia exists as Cr_2O_3, and as μmol $CrO_{1.5}$ referred to mass or BET surface area, respectively.

TPR profiles of some samples are shown in Fig. 1. Pure TiO_2 did not show any significant H_2 consumption. For the chromia catalysts a prominent peak was found at 573–578 K, which shifted to higher temperatures with increasing loading. A second maximum appeared at 680–710 K. The relative amount of H_2 corresponding to the second peak did not exceed 5% of the total consumption and decreased with increasing chromia content. The specific total hydrogen consumptions determined by TPR (both peaks included) are listed in Table 1 (H_2-TPR) for all CrO_x/TiO_2 catalysts. As only CrO_x is reduced, the consumption of H_2 can be expressed as an average decrease of the oxidation state (ΔOS) of Cr. The ΔOS values of 2.2 to 2.7 listed in Table 1 indicate a considerable reducibility of the CrO_x species. Above 5 wt% loading increasing CrO_x contents yield lower ΔOS, which indicates lower relative amounts of higher oxidized CrO_x species after calcination.

In order to gain information about the decomposition (Fig. 2) and the redox behavior, thermoanalytical (TG,

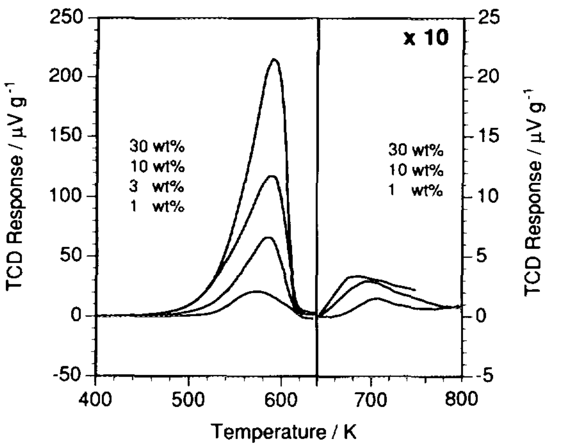

FIG. 1. TPR profiles of chromia on titania catalysts. In order of rising main peak maximum: catalyst carrier (TiO_2, no consumption), 1 wt%, 3 wt%, 10 wt%, and 30 wt% Cr_2O_3. The hydrogen consumption is represented by the TCD response in μV g^{-1}.

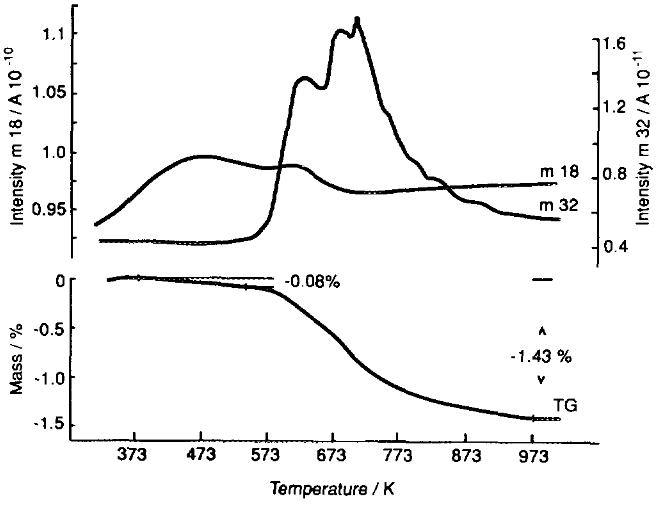

FIG. 2. Decomposition of 10 wt% chromia/titania under an argon atmosphere studied by thermogravimetry (TG) combined with mass spectroscopy (MS) (*m/e* = 18, 32). The sample was previously calcined for 3 h under an oxygen atmosphere at 523 K. MS data are reported as the ion currents of the corresponding masses.

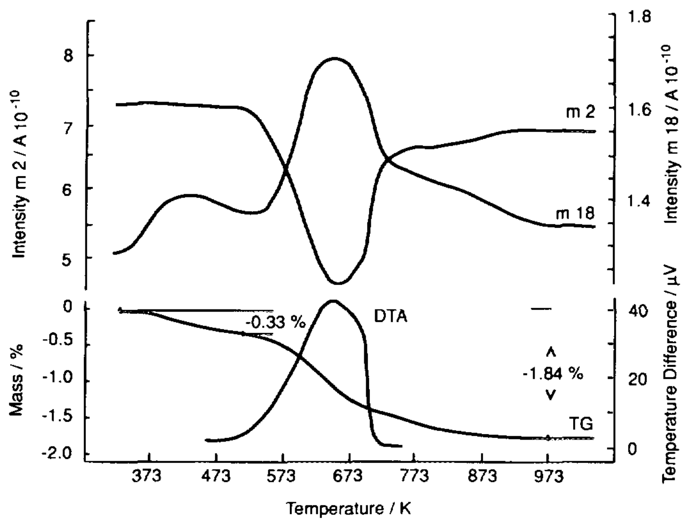

FIG. 3. Reduction behavior of 10 wt% chromia/titania sample under a hydrogen-containing atmosphere (6% H_2/Ar) studied by TG and DTA combined with MS. The sample was previously calcined for 3 h under an oxygen atmosphere at 523 K. Intensities (MS) are reported as ion currents of the corresponding masses. Temperature differences (DTA curve) between sample and reference (50 mg of α-Al_2O_3) are expressed in μV for Pt 10% Rh–Pt thermocouple.

DTA) measurements were carried out with the 10 wt% sample calcined at 523 K in oxygen for 3 h. During decomposition under an argon atmosphere the main species evolving was oxygen, accompanied by evolution of adsorbed water below 670 K (main broad maximum at 470 K, lower maximum at 620 K). The oxygen evolution showed two maxima at 620 K and 690 K and was complete at 920 K. The loss of weight due to oxygen evolution was 1.3%, corresponding to 0.3 mol O_2 per mol Cr assuming total decomposition of CrO_x species to Cr_2O_3.

Figure 3 depicts the reduction behavior measured by thermal analysis using the same gas composition as used for TPR. A similar shape of the reduction profiles is observed as in TPR (Fig. 1). Due to the different calcination temperatures of the samples used for thermal analysis (523 K) and TPR (573 K), the amount of Cr species with valence (V) or (VI) was smaller in the thermoanalytical investigations, leading to a smaller weight loss than expected from the hydrogen consumption measured in TPR. During catalyst reduction, water (m/e = 18) evolved in three discernible steps. Below 570 K mainly adsorbed H_2O evolved, resulting in a weight loss of 0.3%. The prominent peak spanning from 570 K and 720 K is due to water originating from the exothermal reduction of surface species by hydrogen (m/e = 2). This process is partially overlapped by the third significant evolution of water which occurred in a wide temperature range up to 970 K. The total weight loss during thermal analysis up to 1073 K amounted to 1.8%.

The water, which evolved between 570 and 970 K, corresponds to 1.5 wt% of the catalyst. In the temperature range from 720 to 970 K the total water which evolved from the system exceeded the hydrogen consumption significantly. This behavior indicates the formation of $CrO_x(OH)_y$ species and their subsequent dehydration at higher temperatures.

To obtain a high amount of the $CrO_x(OH)_y$ species two other 10 wt% samples were isothermally reduced for 3 h at 693 K in Ar containing 6% H_2. One of the samples was subsequently heated under Ar atmosphere. Water evolved with two distinguishable maximum rates around 620 and 820 K. Each evolution resulted in a weight loss of approximately 0.1%. Small amounts of oxygen evolved between 720 and 1020 K causing a loss of 0.05 wt% (not shown). The other sample was reoxidized in air at 673 K for 1 h. The thermal analysis of this sample in Ar atmosphere (Fig. 4) shows the evolution of oxygen between 580 and 1020 K with a maximum rate at 780 K causing a loss of 0.6 wt%. No water evolved above 570 K. Note that the water which evolved below 570 K had been adsorbed after the pretreatment during the transfer of the sample.

Properties of Catalysts after Use in SCR

The calcined samples with chromia contents of 0.5, 2, and 10 wt% were exposed to SCR feed gas at temperatures up to 620 K for several hours or days. The EPR spectrum of the 0.5 wt% sample measured immediately after this treatment consists of two superimposed powder spectra

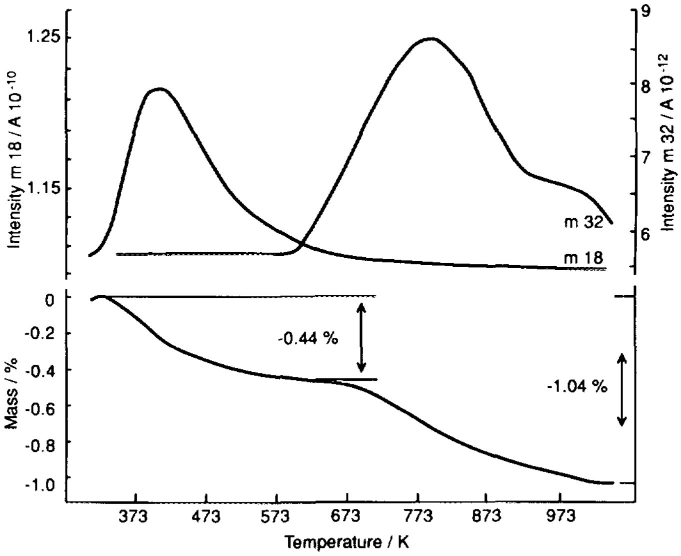

FIG. 4. Oxygen and water evolution from 10 wt% chromia/titania sample. The calcined sample was first reduced for 3 h at 693 K under a hydrogen-containing atmosphere (6% H_2/Ar) and then reoxidized in air at 693 K for 1 h.

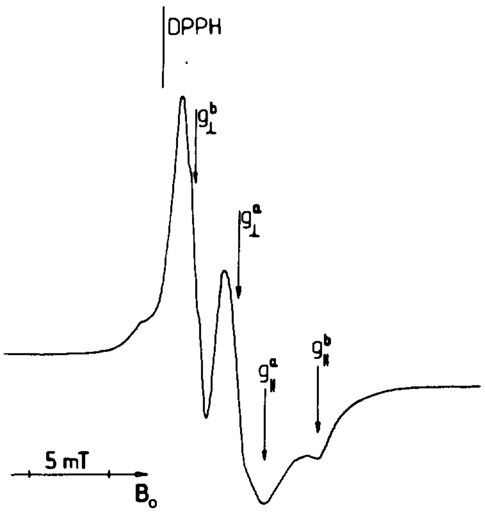

FIG. 5. EPR spectrum of the chromia/titania catalyst (0.5 wt%) after SCR (10 h T_{max} = 400 K), T = 293 K; assignment: (a) Cr^{5+} (γ-signal), (b) $\{CrNO\}^{2+}$.

(Fig. 5). Spectrum (a) is identical with the Cr(V) γ-signal ($g_\perp = 1.974, g_\parallel = 1.959$), whereas spectrum (b) is characterized by a comparatively large g anisotropy (axial symmetry): $g_\perp = 1.989$, $g_\parallel = 1.944$, $A_\perp$ (^{53}Cr) = 17×10^{-4} cm^{-1}. In the "perpendicular part" a hyperfine triplet with $A_\perp = 5 \times 10^{-4}$ cm^{-1} is indicated (interaction with one nucleus $I = 1$, ^{14}N). The same g tensor parameters were derived from the analysis of the Q-band spectra. Identical spectra were obtained by the use of NH_3 (T = 473 K) instead of SCR feed gas. Using NO as feed gas, only the γ-signal was observed. The temperature dependence of the intensity of the powder spectra (Fig. 6) is similar as striking as that of the γ-signal after calcination (antiferromagnetic exchange coupling, discussed in Ref. (14)). For high receiver gain, a broad β-signal (ΔB_{pp} = 70 mT, X-band) superimposed by the spectra described above is observed. In the spectra for higher Cr content, this Cr(III) β-signal clearly dominates. The linewidths of the β-signal, however, are equal for all samples, indicating about the same average cluster size of (amorphous) Cr_2O_3 for all chromia contents: ΔB_{pp} = 70 mT (60 mT for Q-band) at room temperature and 85 (70) mT at T = 130 K. The size of chromium(III) clusters seems to be uniform and too small to show collective magnetic properties (amorphous) for all total chromia contents. For 10 wt%, additionally, some amount of Cr(III) incorporated into the rutile lattice is observed. The Cr(VI) content is remarkably reduced by SCR treatment as deduced from experiments with ethylene glycol (see Ref. (14)).

Based on chemistry and spectroscopy, we interpret spectrum (b) as arising from $\{Cr^INO\}^{2+}$ surface complexes. The EPR parameters agree well with those of comparable Cr(I) nitrosyl complexes ($3d^5$, "low-spin," $S = \frac{1}{2}$ (19). It is known from chromium chemistry that Cr(VI) forms $\{Cr^INO\}^{2+}$ complexes by reaction with hydroxylamine (20). A similar reaction with gaseous NH_3 is well imaginable. Analogous complexes were observed by EPR and FTIR on Cr(III)-exchanged zeolites reduced by H_2 upon adsorption of NO (21). The reductively pretreated chromia/titania catalysts (H_2, 573 K) show only traces of Cr(V) (γ-signal) after SCR, but do not show the signal assigned to $\{Cr^INO\}^{2+}$ by us.

Catalytic Behavior

The catalytic behavior of the various catalysts in the selective reduction of NO has been tested and the results are listed in Table 2. The selectivity to undesired N_2O is given for two different temperatures (423 and 453 K) because the catalysts showed NO conversion in temperature ranges which only partially overlap. The kinetics are characterized by the nitric oxide reaction rate at 423 K referred to the BET surface area, by the turnover frequency (TOF) at 423 K expressed as NO molecules, which reacted per chromium atom, and by the apparent activation energy E_a for the NO conversion.

Temperatures at which NO conversion reached 50% ($T_{X_{NO}=0.5}$) provide an additional measure for the activities of the catalysts. Note that these temperatures decrease from 527 to 421 K when the chromia loading increases from 0.5 to 30 wt%. A pronounced decrease in $T_{X_{NO}=0.5}$ is observed when the chromia loading is increased from 0.5 to 3 wt%, while a further increase of the chromia loading has only a minor effect. Complete conversion of ammonia was achieved at a temperature of 463 K for the 30 wt% chromia/titania catalyst together with a maximum NO

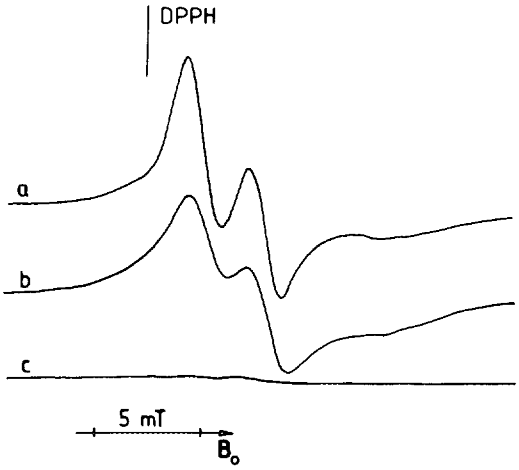

FIG. 6. Temperature dependence of the EPR spectrum of the chromia/titania catalyst (0.5 wt%) after SCR: (a) T = 413 K, (b) 293 K, and (c) 130 K (identical recording parameter).

TABLE 2

Results of SCR Activity Measurements

Sample	Conversion $T_{X_{NO}=0.5}$ (K)	$Rate_{NO,423\ K}$ (10^{-9} mol s^{-1} m^{-2})	$TOF_{423\ K}$ (10^{-5} $NOCr^{-1}$ s^{-1})	$E^*_{a\,NO}$ (kJ mol^{-1})	ln k_{0NO} (mol cm^{-3} s^{-1})	$S_{N_2O,453\ K}$	$S_{N_2O,423\ K}$
0.5 wt%	527[a]	0.2	15[b]	—	—	0.23[a]	—[a]
1 wt%	501	0.5	19	51 ± 2[c]	10.5	0.24	—
2 wt%	467	1.2	21	47 ± 2	10.2	0.22	—
3 wt%	448	2.0	23	47 ± 2	11.0	0.17	0.09
5 wt%	438	2.8	21	51 ± 3	12.1	0.16	0.08
10 wt%	433	4.3	16	52 ± 2	13.1	0.17	0.08
30 wt%	421	6.6	8	51 ± 4	13.4	0.16	0.07
Amorphous Cr_2O_3	388	3.1	(4.6)	50 ± 2	9.8	—	0.10
V_2O_5/TiO_2	448	2.2	39[d]	56 ± 4	—	<0.01	<0.01
5 wt%; H_2 653 K	427	2.9	22	45 ± 1	10.6	0.08	0.03
5 wt%; H_2 723 K	441	2.4	18	42 ± 2	9.5	0.02	0.01

[a] Determined at constant GHSV of 24,000 h^{-1} for all samples.
[b] TOF based on total amount of Cr in catalyst.
[c] 95% confidence limits of Arrhenius-type linear regression.
[d] TOF based on total amount of V in catalyst.

conversion of 81%. The corresponding values for the 10 and 0.5 wt% catalysts were 486 K, 82% and 543 K, 70%, respectively. The rate of NO reaction referred to the total surface area increases almost linearly with the chromia loading up to 5 wt%, as emerges from the rate versus chromia content plot shown in Fig. 7. A further increase of the loading appears to be less effective. Compared to the 5 wt% sample, the 10 wt% catalyst shows a 1.6-fold greater rate of NO conversion and the 30 wt% catalyst a 2.4-fold greater rate. The rates of NO conversion referred to surface or mass are plotted together with results of the two reference samples (amorphous chromia and V_2O_5/TiO_2) in the Arrhenius-type plots shown in Fig. 8. The TOF values (Table 2), all around 20 × 10^{-5} s^{-1} for the 1 to 5 wt% samples, pass through a maximum at a chromia loading of 3 wt%. The lower TOF values for the 0.5 and the 10 and 30 wt% samples indicate that the chromia species of these catalysts are either less active or less accessible for NO conversion. The selectivity to undesired N_2O decreases with increasing chromia loading up to 3 wt%. Higher loading has no further influence on the selectivity. For the higher loaded samples, selectivities comparable to that of amorphous chromia (6) were found. It is noteworthy to mention that during a long term activity test under SCR conditions for 150 h at temperatures between 420 and 520 K, a 5 wt% sample did not show any deactivation.

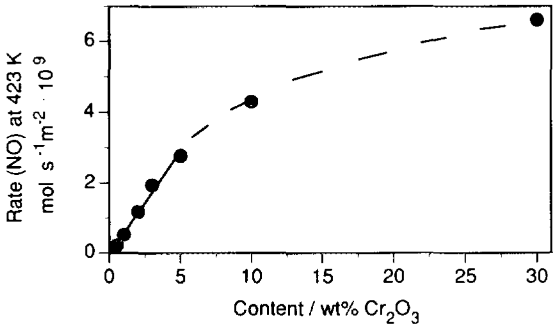

FIG. 7. Increase of specific rate of nitric oxide conversion at 423 K as a function of the chromia loading. Catalyst pretreatment was 3 h in oxygen at 573 K.

Using hydrogen (6% H_2 in Ar) and temperatures higher than 570 K for the pretreatment, the 5 wt% sample reached a higher activity than the corresponding oxidatively calcined catalyst. The highest activity was obtained with the catalyst pretreated at 653 K. $T_{X_{NO}=0.5}$ was lowered by 11 K and the rate of NO conversion and TOF values were increased. This increase of the activity emerges also from the results shown in the top two sections of Fig. 9, where the conversions of NO and NH_3 are plotted as a function of temperature for differently pretreated 5 wt% chromia/titania samples. Pretreatment at 723 K in H_2/Ar lowered the activity to slightly below the one obtained by calcination. After further heating in an argon atmosphere up to 873 K (2 h), the activity is significantly lower as shown, in the X vs T plots (Fig. 9). The starting activity (until conversion corresponding to a steady-state had been established in the reactor; i.e., after ca 2 h at 423 K) also depended on the pretreatment. After reaching a maximum starting activity within a few minutes (high NO and NH_3 conversion), it decreased to a steady state activity in the case of reductively pretreated catalysts, whereas after O_2 calcination during a starting period (ca 20 min) total NH_3 consumption together with gradually rising NO conver-

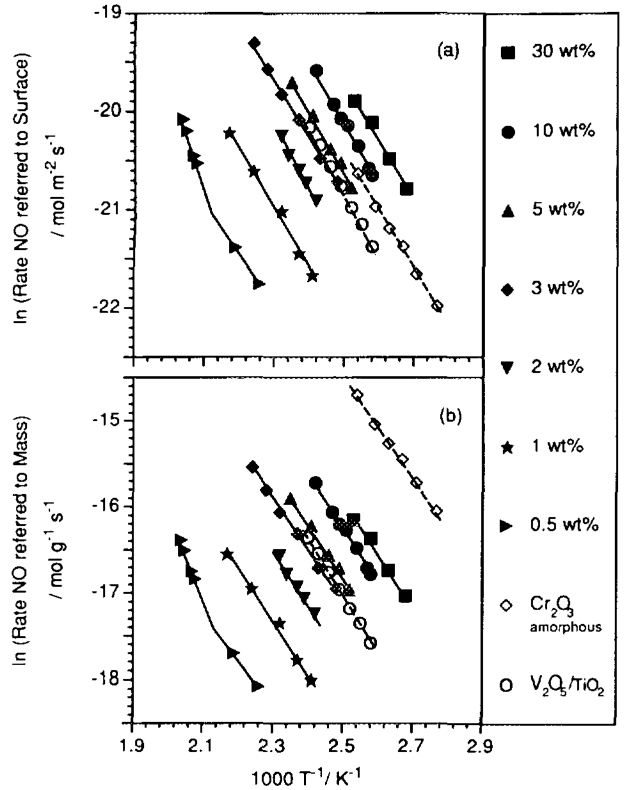

FIG. 8. Arrhenius-type plots of the rates of nitric oxide reaction at maximum 20% NO conversion for the entire series of chromia/titania catalysts (full lines). Reference catalysts: amorphous chromia and the V_2O_5/TiO_2 catalyst (dotted lines). (a) Rates referred to the BET surface area of the catalysts. (b) Rates referred to the mass of the catalyst.

sion was monitored. The selectivity to N_2O decreased significantly upon reductive pretreatment compared to the oxidatively calcined catalysts (Fig. 9 and Table 2). With the sample pretreated in H_2/Ar at 723 K and the one which was subjected to further annealing in Ar, the concentration of N_2O detected in the product stream did not exceed 12 ppm in the temperature range up to 463 K. This concentration was slightly above the limit of detection (5 ppm).

The values for the apparent activation energy E_a for NO conversion were calculated from the Arrhenius-type linear regression of the data shown in Fig. 8. E_a values of 47 to 52 kJ · mol^{-1} were obtained. The kinetic data of the 0.5 wt% catalyst did not fit an Arrhenius-type regression, indicating the competition of at least two reactions in the temperature range 420–490 K. For the catalysts which had been pretreated in hydrogen, slightly lower E_a values were found.

DISCUSSION

For the chromia/titania catalysts after calcination, the presence of large amounts of chromia of higher valence states can clearly be deduced from the hydrogen consumption during TPR. This represents further support for the results of Part I (14), where the coexistence of (at least) the oxidation states +3, +5, and +6 was found subsequent to calcination. These findings are also in agreement with the results of other authors for chromia supported on different carrier oxides (12, 22–24), where Cr(VI) was found to form the predominant surface species up to a certain saturation coverage strongly dependent on the carrier oxide (TiO_2, Al_2O_3, SiO_2, ZrO_2). Higher loadings resulted in the partial formation of α-Cr_2O_3 crystallites on all carrier materials, as also found by us for titania (14).

The TPR profiles shown in Fig. 1 indicate that the catalysts were reduced in two stages. An average decrease

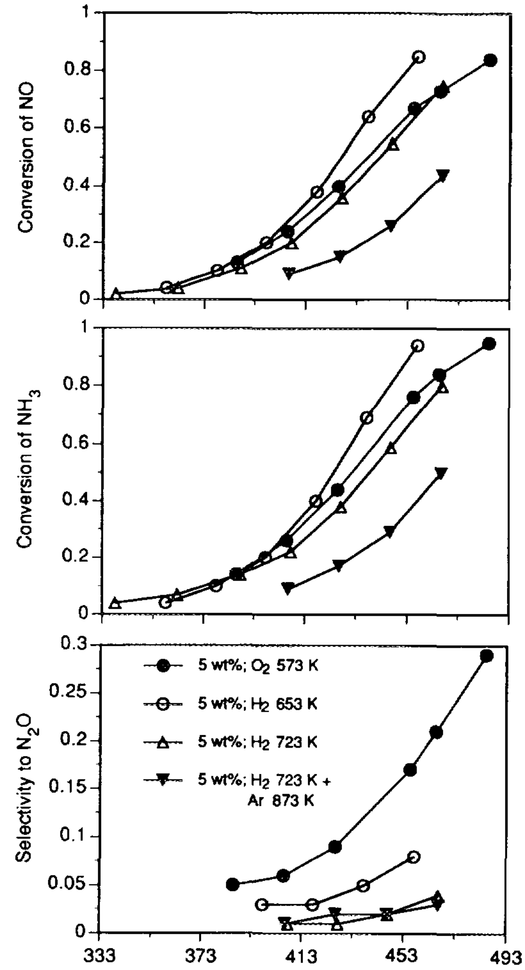

FIG. 9. Conversions of nitric oxide and ammonia and selectivity to nitrous oxide as a function of temperature for differently pretreated 5 wt% catalysts. The pretreatments were: (●) Calcination for 3 h in oxygen at 573 K. (○) *In situ* calcination in 6% hydrogen/argon for 3 h at 653 K. (△) *In situ* calcination in 6% hydrogen/argon for 2 h at 723 K. (▼) Further annealing in argon for 2 h at 873 K.

of the oxidation state, ΔOS, of between 2 and 3, as found for low and moderate chromia contents (Table 1), would correspond to the total reduction of all Cr(V) and Cr(VI) species to Cr(III). The lower total hydrogen consumption for moderately and highly loaded samples confirms the existence of larger Cr(III) fractions in the calcined catalysts, which likewise agrees well with the EPR results (14).

Very similar TPR behavior was found for chromia supported on alumina by Grünert *et al.* (12, 25). They obtained ΔOS values between 2.35 for low and 1.4 for high chromia loadings. The formation of Cr valences lower than +3 during the high temperature reduction ($T > 640$ K), as proposed by Grünert for a small part of the Cr on Al_2O_3, cannot be excluded for our system. Only a small part of the Cr(III) seems to be accessible for further reduction as the maximum contribution due to high temperature reduction indicates (5% of total H_2 consumption; 1 wt% sample).

The hydrogen consumption profile obtained by thermal analysis (TG, DTA; $m/e = 2$, Fig. 3) is in agreement with the TPR profile. The difference of hydrogen consumption (little) and evolution of water (pronounced) from the system at temperatures between 725 and 1000 K indicates that the hydrogen uptake (525–725 K) is accompanied by the formation of hydrogen-containing species in the catalyst. This behavior can be attributed to two different processes, namely to the hydroxylation of dispersed $Cr(III)O_x$ surface species on the one hand and the formation of a hydrogen-containing $Cr(III)O_x(OH)_y$ phase, e.g., CrOOH, on the other.

The interconversion of orthorhomic CrOOH and tetragonal CrO_2 was summarized by Alario-Franco and coworkers (26, 27) in the following scheme:

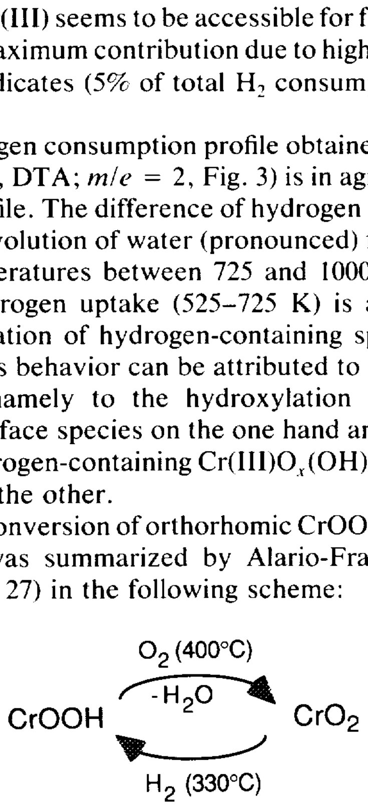

After partial decomposition of CrO_2 to Cr_2O_3, only the non-α-Cr_2O_3 part was accessible for reoxidation.

The comparison of TPR and decomposition under an Ar atmosphere using thermoanalytical methods (Fig. 2) showed that the evolution of oxygen takes place in the same temperature range as the reduction in a hydrogen atmosphere, but it could be resolved into two steps. The small difference in the weight loss compared to the reduction in hydrogen (decomposition of CrO_x: −1.35%; reduction: −1.51%) is caused by the difference in the final oxidation state and by the incompleteness of the decomposition, respectively. As already mentioned, it is assumed that the final oxidation state of chromium is +3. The appearance of two discrenible steps could represent, e.g., the formation of Cr(V) surface complexes, which have been shown to be stable on the TiO_2 surface after calcination, and the subsequent reduction of the Cr(V) to Cr_2O_3. Solid state reactions such as the incorporation of cations into the TiO_2 are supposed to occur favorably above 900 K and have to be taken into account as well. The superimposition of several processes leading to a possible evolution of oxygen may explain the long tailing of the oxygen evolution curve observed in Fig. 2.

The formation of reoxidizable $Cr(III)O_x(OH)_y$ in calcined chromia catalysts during exposure to H_2/Ar at moderate temperatures (690 K) was evidenced by the additional thermoanalytical experiments. The nature of the reoxidized species cannot be further assigned, but the possibility of partial reoxidation after reduction in hydrogen is pointed out. The reoxidation of the chromia on titania seems to be possible, as long as neither α-Cr_2O_3 is formed nor Cr(III) is incorporated into the support.

The uniform size of the Cr(III) clusters after SCR for all loadings deduced from EPR indicates that the small α-Cr_2O_3 crystallites, monitored in the calcined 10 wt% sample, had been decomposed by SCR. This demonstrates the high mobility and the ease of oxidation/reduction processes of chromia supported on TiO_2 under SCR conditions.

The catalysts used in this work exhibit high activity for SCR in the low temperature range (420–470 K), and the NO conversion rate of the calcined samples rises almost linearly with the chromia loading up to 5 wt%. A further increase of the loading enhances the NO reaction rate per unit surface area slightly, but is less effective with regard to the TOF. At the same loadings crystallites of α-Cr_2O_3 have been found in the calcined samples. The capacity of a theoretical monolayer of Cr_2O_3 on the titania support (P25) calculated from the area need of a virtually cubic cell of one Cr atom would be in the same range (8.25 wt%). Taking into account the different reaction conditions, the results of our calcined catalysts are in good qualitative agreement with X_{NO} versus temperature characteristics as well as the product distribution reported by Wong and Nobe (2) for a chromia on titania catalyst. The distinct increase of the N_2O production at 480 K, described by them for a 10 wt% catalyst, was found for all chromia concentrations in our system.

A comparison of the NO reaction rates using the Arrhenius-type plots (Fig. 8) shows that the favourable properties of the bulk amorphous CrO_x are mainly based on the four times higher specific total surface area compared to that of the TiO_2 (P25) supported catalysts. If the reaction rate is referred to the surface area, the supported systems reach at the saturation coverage the same activity as the amorphous chromia. Activation energies of 50 ± 5 kJ mol^{-1} are typical for SCR (2). The slightly lower activation energies observed after reductive pretreatment correspond to results found by Curry-Hyde *et al.* for amorphous chromia (6).

The selectivity to undesired N_2O was higher for low chromia concentrations than for loadings of at least 3 wt%. As there is no significant change in the selectivity characteristics from 3 to 30 wt%, it is stated that the selectivity is independent of the chromia concentration. This is in agreement with the observation of uniformly sized chromia clusters after exposure to SCR conditions for this range of chromia concentrations.

Based on the results of this study, no mechanism for the formation of N_2O on chromia/titania can be suggested. The kinetic measurements indicate a stronger temperature dependence (higher activation energy, typically 100 ± 10 kJ mol^{-1}) for the formation of N_2O compared to N_2 production (40 ± 5 kJ mol^{-1}). However, similar temperature dependences were found for the consumption of NO and NH_3. Therefore the source of N_2O formation cannot be determined unambiguously. Investigations of NH_3 oxidation in the absence of NO and of NO reduction with NH_3 in the absence of O_2, as made in Ref. (17) for pure chromia samples, as well as isotope labelling of the reactants, could provide further information about the source of N_2O.

In particular, the selectivity and the initial activity of the titania-supported chromia catalysts depend markedly on the pretreatment. In the series of reductive pretreatments at temperatures below 720 K, an improved selectivity to N_2 of >90% was found for reaction temperatures up to 470 K without loss of the NO reaction rate. The lowering of the activity due to further annealing in Ar at 873 K is attributed to the partial crystallization of α-Cr_2O_3 and to the incorporation of Cr(III) into titania. These two processes have been proposed above to limit the reoxidizability of the Cr(III) species as well.

The improved selectivity and the higher starting activity due to reductive pretreatment at moderate temperatures can be discussed in the context of the reduction of Cr(VI) and Cr(V) surface species, taking place during such a pretreatment, and in the context of the hydroxylation of the Cr(III) surface species.

In the case of samples calcined in O_2, Cr(VI) complexes cover Cr(III) species partially or completely (14). At the beginning of the SCR experiment, NH_3 is consumed to reduce Cr(VI) to give, e.g., $\{Cr^{I}NO\}^{2+}$ surface complexes, which is in agreement with the analysis of the gases leaving the reactor. The resulting Cr(I) complexes are obviously stable under SCR conditions and as a result possibly block catalytically active sites. On the catalysts subjected to reductive pretreatment, no Cr(VI) is present and, consequently, Cr(I) is neither expected to be formed, nor found. Active sites are not blocked and no NH_3 is consumed for the reduction of undesired Cr(VI) at the beginning of the reaction. This leads to an increased starting activity.

Hydroxylated Cr(III) species formed during reductive pretreatment represent potential Brønsted acid sites when located at the surface. Such sites have been proposed to be the main active sites for SCR on vanadia/titania catalysts by Topsøe (28). The question remains of whether $CrO_x(OH)_y$ species are stable under SCR reaction conditions and how they contribute to the catalytic activity. As no *in situ* vibrational spectroscopy was used in this study, all correlations of reactivity characteristics with *ex situ* observations (e.g., thermal analysis, TPR, EPR) need further *in situ* investigations for evidence. Temperature programmed reaction and desorption (TPRD) studies, combined with *in situ* FTIR, will be presented in a forthcoming paper (29).

ACKNOWLEDGMENTS

Thanks are due to Dr. M. Maciejewski for carrying out the thermal analytical studies. Financial support by the Swiss National Science Foundation (NFP 24) is kindly acknowledged.

REFERENCES

1. Bosch, H., and Janssen, F., *Catal. Today* **2,** 369 (1988).
2. Wong, W. C., and Nobe, K., *Ind. Eng. Chem. Prod. Res. Dev.* **25,** 179 (1986).
3. Niiyama, H., Murata, K., Ebitani, A., and Echigoya, E., *J. Catal.* **48,** 194 (1977).
4. Kobylinski, T. P., and Taylor, B. W., *J. Catal.* **31,** 450 (1973).
5. Curry-Hyde, H. E., and Baiker, A., *Ind. Eng. Chem. Res.* **29,** 1985 (1990).
6. Curry-Hyde, H. E., Musch, H., and Baiker, A., *Appl. Catal.* **65,** 211 (1990).
7. Curry-Hyde, H. E., Musch, H., Schraml-Marth, M., Wokaun, A., and Baiker, A., *J. Catal.* **133,** 397 (1992).
8. Schraml-Marth, M., Wokaun, A., Curry-Hyde, H. E., and Baiker, A., *J. Catal.* **133,** 415 (1992).
9. Schraml-Marth, M., Wokaun, A., Curry-Hyde, H. E., and Baiker, A., *J. Catal.* **133,** 431 (1992).
10. Schraml-Marth, M., Wokaun, A., and Baiker A., *J. Catal.* **138,** 306 (1992).
11. Merryfield, R., MacDaniel, M., and Parks, G., *J. Catal.* **77,** 384 (1982).
12. Grünert, W., Shipiro, E. S., Feldhaus, R., Anders, K., Antoshin, G. V., and Minachev, K. M., *J. Catal,* **100,** 138 (1986).
13. Hardcastle, F. D., and Wachs, I. E., *J. Mol. Catal.* **46,** 173 (1988).
14. Köhler, K., Schläpfer, C. W., von Zelewsky, A., Engweiler, J. Nickl, J., and Baiker, A., *J. Catal.* **143,** 201 (1993).
15. Kijenski, J., Baiker, A., Glinski, M., Dollenmeier, P., and Wokaun, A., *J. Catal.* **101,** 1 (1986).
16. Monti, D. A. M., and Baiker, A., *J. Catal.* **83,** 323 (1983).
17. Curry-Hyde, H. E., and Baiker, A., *Appl. Catal.* **90,** 183 (1992).
18. Barrett, E. P., Joyner, L. G., and Halenda, P. P., *J. Am. Chem. Soc.* **73,** 373 (1951).
19. Goodman, B. A., Raynor, J. B., and Symons, M. C. R., *J. Chem. Soc.* (*A*), 1973 (1968).
20. Griffith, W. P., *J. Chem. Soc.* 3286 (1963).
21. Naccache, C., and Ben Taarit, Y., *J. Chem. Soc. Faraday Trans. I* 1475 (1973).

22. Hardcastle, F. D., and Wachs, I. E., *J. Mol. Catal.* **46,** 173 (1988).
23. Kim, D., Tatibouet, J.-M., and Wachs, I. E., *J. Catal.* **136,** 209 (1992).
24. Martin, C., Martin, I., Rives, V., Palmisano, L., and Schiavello, M., *J. Catal.* **134,** 434 (1992).
25. Grünert, W., Shipiro, E. S., Feldhaus, R., Anders, K., Antoshin, G. V., and Minachev, K. M., *J. Catal.* **99,** 149 (1986).
26. Alario-Franco, M. A., and Sing, K. S. W., *J. Therm. Anal.* **4,** 47 (1972).
27. Sáez-Puche, R., and Alario-Franco, M. A., *J. Solid State Chem.* **47,** 59 (1983).
28. Topsøe, N.-Y., *J. Catal.* **128,** 499 (1991).
29. Schneider, H., Scharf, U., Wokaun, A., and Baiker, A., submitted for publication.